



HAL
open science

On the thermal aging of a filled butadiene rubber

Komla Dela Ahose, Stéphane Lejeunes, Dominique Eyheramendy, Franck Sosson

► **To cite this version:**

Komla Dela Ahose, Stéphane Lejeunes, Dominique Eyheramendy, Franck Sosson. On the thermal aging of a filled butadiene rubber. 10th European Conference on Constitutive Models for Rubber (ECCMR2017), Aug 2017, Munich, Germany. pp.59-64, 10.1201/9781315223278-8 . hal-01586866

HAL Id: hal-01586866

<https://hal.science/hal-01586866>

Submitted on 18 Apr 2018

HAL is a multi-disciplinary open access archive for the deposit and dissemination of scientific research documents, whether they are published or not. The documents may come from teaching and research institutions in France or abroad, or from public or private research centers.

L'archive ouverte pluridisciplinaire **HAL**, est destinée au dépôt et à la diffusion de documents scientifiques de niveau recherche, publiés ou non, émanant des établissements d'enseignement et de recherche français ou étrangers, des laboratoires publics ou privés.

On the thermal aging of a filled butadiene rubber

K.D. Ahoſe & S. Lejeunes & D. Eyheramendy

LMA, Aix-Marseille Univ., Centrale Marseille, CNRS UPR7051, F-13402 Marseille Cedex 20, France

F. Sosson

SMAC, 83079 Toulon Cedex 9, France

ABSTRACT: In this study we investigate the influence of thermal aging on the mechanical properties of a butadiene rubber filled with carbon black. To emphasize the influence of both the crosslink density and the crosslink lengths, we consider three different materials based on the same formulation. Dynamic and quasi-static characterizations are realized periodically at room temperature to study of the impact of aging on various mechanical characteristic such as the equilibrium hysteresis, the Payne effect, etc. Crosslink density is followed by swelling tests.

1 INTRODUCTION

The impact of thermal aging phenomena on physical properties such as mechanical stiffness, tensile strength limit, loss angle, shore hardness, has been studied by many authors, see for instance Tomer, Delor-Jestin, Singh, & Lacoste 2007, Shabani 2013, Kumar, Commereuc, & Verney 2004, Kartout 2016, Ben Hassine 2013 and references therein. Obviously, aging phenomena are material dependent and different issues arise depending on monomers or vulcanizate agents (see Choi, Kim, & C.-S. 2006 for a comparison of EPDM and NBR). These phenomena are also strongly coupled with the environment, chemical reactions can occur with air (oxidation), salt water (see for instance Gac, Saux, Paris, & Marco 2012, Rabanizada, Lupberger, Johlitz, & Lion 2015), etc. Furthermore, mechanical state during thermal aging may also have an influence on aging phenomena (see for instance Ciutacu, Budrugaec, Mare, & Boconcios 1990). The chemo-physical evolutions involved during aging may lead both to the formation of new crosslinks and to the dissociation of existing ones. For sulfur vulcanized system a commonly admitted mechanism is the degradation of poly-sulfur crosslinks into di-sulfur or mono-sulfur ones. Free sulfurs can eventually migrate and form new crosslinks. This phenomenon is of interest for mechanicians as it can occur during high-cycles fatigue in particular when the heat-build is significant or when the thermal environment plays an important role.

In this study we propose to investigate the consequence of thermal aging on a butadiene rubber

reinforced with carbon black fillers and vulcanized with sulfur. To study the influence of the poly-sulfur crosslinks we consider a single rubber formulation cured under different conditions (temperature and time of cure). This leads to different crosslink networks and different crosslink densities. We proceed to mechanical characterizations with quasi-static and dynamic tests on unaged and aged specimens.

2 EXPERIMENTAL SETUP

2.1 Materials

The material is a polybutadiene rubber reinforced with carbon black and vulcanized with sulfur. Due to confidentiality reasons, the formulation of this rubber can not be detailed here. The vulcanization system is efficient (sulfur to accelerator ratio is greater than one) and the filler mass fraction is about 45%. This system was cured at three different temperatures: 130°C, 150°C and 170°C. The time of cure for each temperature was previously determined with the help of a rheometer: time of cure was obtained when the measured torque reached 98% of the maximum observed one at each temperature. We obtained the following time of cure: 170°C – 7min, 150°C – 17min, 130°C – 55min. To simplify, in the following each couple time/temperature is referred to as a different material even if the initial composition is the same. Each material can be considered as fully vulcanized and differs from each other from its network structure: for high temperature, we have higher crosslink lengths (poly-sulfurs) and a smaller crosslink density

than for smaller temperatures of cure.

2.2 Thermal aging

Thermal aging of H2 tensile specimens was done with the help of an oven. Each sample was previously put inside an individual plastic bag in which air was partially removed with a vacuum pump. The objective was to minimize thermo-oxidative phenomena and to limit non homogeneous aging. Some specimens, 2 by material, were periodically removed from the oven for mechanical, and chemical characterizations at room temperature.

2.3 Mechanical characterizations

Mechanical characterizations on tensile specimen consisted into the following sequence: a softening phase to eliminate the Mullins effect, relaxations by step (relaxations at different increasing and decreasing amplitudes), cyclic sinusoidal tests with two static amplitudes and three dynamics amplitudes (frequencies of $0.1Hz$, $3Hz$, $6Hz$, $10Hz$). These tests were all done at room temperature.

3 UNAGED BEHAVIOR

3.1 Chemical and thermal characterizations

We realized swelling tests on small specimens that were put in xylene. Figure 1, shows the evolution of the relative swelling ratio in mass upon the time spent in solvent. We define the relative swelling ratio in mass from:

$$q = \frac{m_s - m_0}{m_0} \quad (1)$$

where m_s is the mass of the specimen after swelling and m_0 is the initial mass. Swelling tests are good indicators of the crosslink density of the vulcanized network. The crosslink density could be estimated using the equation proposed by Kraus 1963 for filled rubber, however, we do not had access to the volume fraction of unfilled rubber in the swollen rubber phase. Nevertheless, it can be seen from Kraus or Flory-Rhener works (Flory & Rehner 1943) that crosslink density is related to the inverse of the previously defined swelling ratio. We can therefore admit that crosslink density is higher for the material cured at $130^\circ C - 55min$ than for those cured at $150^\circ C - 17min$ and $170^\circ C - 7min$. We also realized thermal characterizations with a DSC and optical dilatometry with DIC. The glass-transition temperature was measured at $-82^\circ C$ for each materials and the thermal dilatation behavior was also very close for each materials.

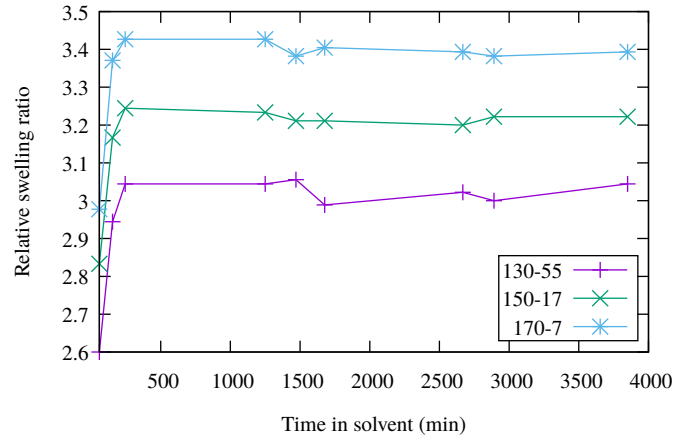


Figure 1: Relative mass solvent absorption upon the swelling time for the three materials on virgin samples (not submitted to thermal aging)

3.2 Mechanical behavior

Figures 2 and 3 show some obtained results on unaged samples. It can be seen that, in accordance with the statistical theory of rubber network, the higher is the crosslink density the higher is the stiffness. Dynamic tests show that the dynamic softening effect (Payne effect) is nearly the same in the three unaged materials, hysteresis area are larger for the material that was cured at $170^\circ C$ that for this at $150^\circ C$, which show also a larger hysteresis area than the one cured at $130^\circ C$, see for instance figure 4.

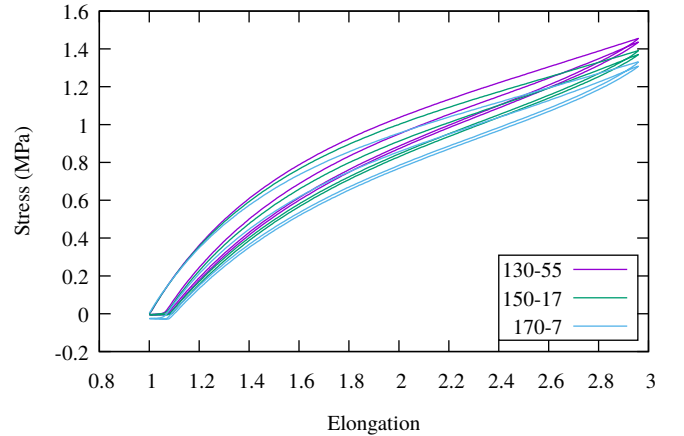


Figure 2: Stress softening in tension on non-aged samples (not submitted to thermal aging)

3.3 Modeling of the unaged behavior

We adopt a modeling framework that is very close to the one of Delattre et al. 2016. The equilibrium part of the stress is considered as hyperelastic and non-equilibrium one is modeled with a series of Maxwell elements (Generalized Maxwell model) with an accounting of the Payne effect as described in Delattre et al. 2016. The Cauchy stress, σ , is therefore defined from:

$$\sigma = \sigma_{eq} + \sigma_{neq} - p\mathbf{1} \quad (2)$$

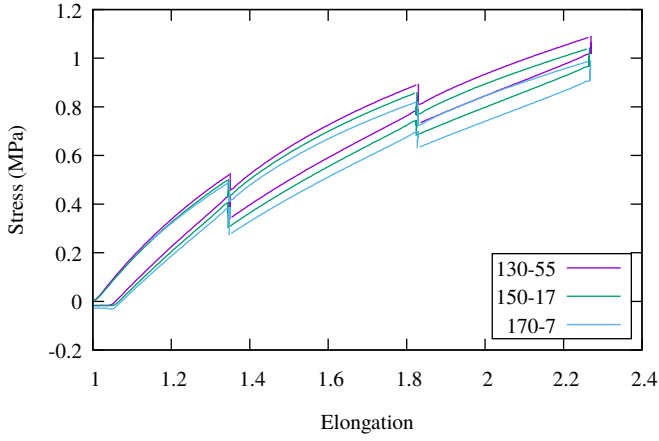


Figure 3: Relaxation by steps in tension on non-aged samples (not submitted to thermal aging)

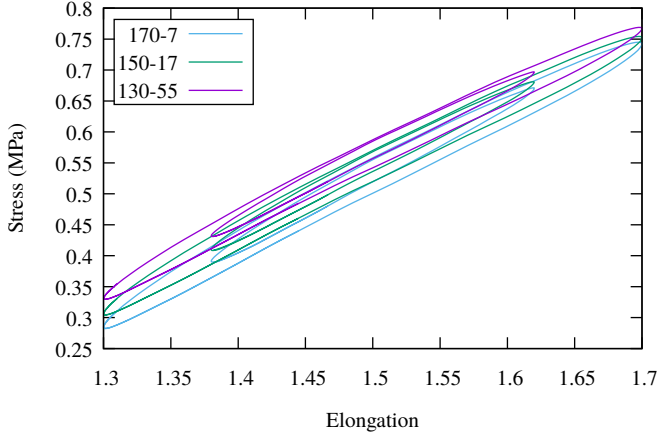


Figure 4: Stabilized hysteresis in tension on non-aged samples for cyclic tests at 3Hz

where p is the hydrostatic pressure. For the equilibrium part, we adopt a Mooney-Rivlin potential defined such as:

$$\rho_0\psi_{eq} = sC_{10}(I_1 - 3) + sC_{01}(I_2 - 3) \quad (3)$$

where ρ_0 is the reference density, I_1, I_2 the two first strain invariants. The material coefficients, C_{10}, C_{01} are classical Mooney parameters (which are identical for each materials) and s is a parameter that is fixed to 1 for the material 130-55 and that is identified for other materials. The identification of $C_{10}, C_{01}, s_{150}, s_{170}$ is done by minimizing the least-square distance from the end of relaxation points (extracted from figure 3) to the predicted ones for the three materials at the same time. We obtain the material parameters given at table 1 (see also figure 5). It can be remarked that the obtained values for s are nearly equal to the inverse of the relative swelling ratio such as we recover the hypothesis of proportionality of the rubber elasticity upon the crosslink density that is made in statistical theories. We can postulate:

$$s_x = \frac{q_{130}}{q_x} \quad (4)$$

where x stands for the material 150-17 or 170-7.

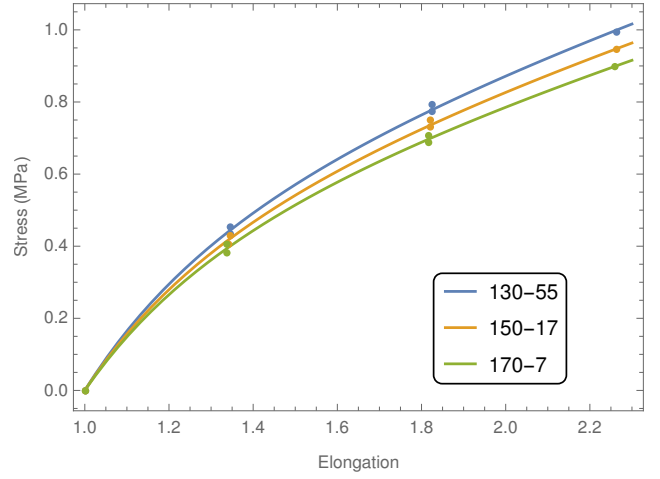


Figure 5: Identification of the equilibrium contribution with a Mooney-Rivlin potential

C_{10}	C_{01}	s_{150}	s_{170}
0.185 MPa	0.127 MPa	0.948	0.9
q_{130}/q_{150}	q_{130}/q_{170}		
0.944	0.898		

Table 1: Material parameters of the equilibrium part

For the non-equilibrium part, we adopt a Neo-Hookean potential and a Maxwell viscous flow:

$$\left\{ \begin{array}{l} \rho_0\psi_{neq} = \sum_{i=1}^n (G_i/s)\omega_i(I_1^{e_i} - 3) \\ \dot{\bar{\mathbf{B}}}_{ei} = \bar{\mathbf{L}}\bar{\mathbf{B}}_{ei} + \bar{\mathbf{B}}_{ei}\bar{\mathbf{L}}^T - \frac{1}{s\tau_i}\bar{\mathbf{B}}_{ei}^D\bar{\mathbf{B}}_{ei} \\ \dot{\omega}_i = -\frac{1}{h_i} \left\langle \omega_i - \left(\frac{3}{I_1(\bar{\mathbf{B}})} \right)^{r_i} \right\rangle, \quad \omega_i(t=0) = 1 \end{array} \right. \quad (5)$$

where $\bar{\mathbf{B}}_{ei}$ is the i^{th} isochoric left Cauchy Green tensor coming from the i^{th} multiplicative split of the transformation gradient into viscous and elastic part, $\bar{\mathbf{L}}$ is the isochoric tensor of eulerian velocities, ω_i is the i^{th} internal variable to account of the Payne effect, and G_i, τ_i, h_i, r_i are material parameters ($i = 1..n$).

The material parameters identification of the non equilibrium part is done only on the data of the material 130-55 (by setting $s = 1$). We have therefore a viscoelastic model that can account of a variation of the crosslink density, using the relation of eq. (4). A good agreement with the response of the two other materials is observed as can be seen from the figures 6 and 7.

4 AGED BEHAVIOR

We investigate, in this section, the behavior of aged tensile samples that were put in a oven at $90^\circ C$. No

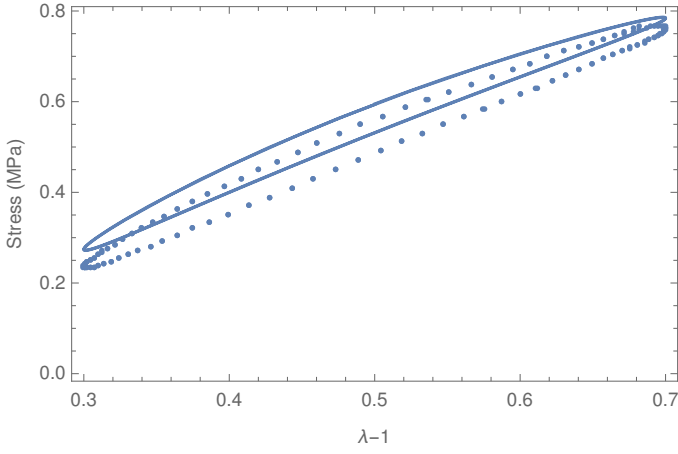


Figure 6: Validation of the identified parameters of the non-equilibrium contribution with the material 170-7 ($f = 10Hz$)

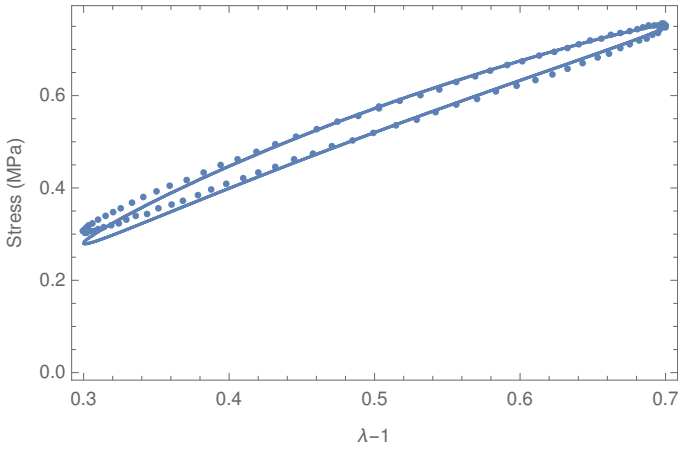


Figure 7: Validation of the identified parameters of the non-equilibrium contribution with the material 150-17 ($f = 3Hz$)

significant variation of mass or volume, of the samples, was observed after aging.

4.1 Chemical characterizations

The results of the swelling tests done at different aging time is synthesized with figure 8. We plotted the inverse of the swelling ratio q relative to the initial (unaged) swelling ratio q_0 for each material. It can be seen that the material that has the larger initial mean crosslink length (the larger number of polysulfur crosslink) exhibits the stronger evolution of the crosslink density. After 11 days of aging, the swelling ratio, q , is very close for each material as the initial concentration of sulfur is the same in each material.

4.2 Mechanical characterizations

To investigate the results of relaxation tests, we have plotted the stiffness obtained from the end of relaxation tests done at the maximum amplitude. It can be seen from figure 9 that the equilibrium behavior become stiffer. Furthermore, the material 170-7 seems to become more rigid than the two others. We can also notice that the dispersion of the results increases with aging.

For dynamic tests, we calculated the median line

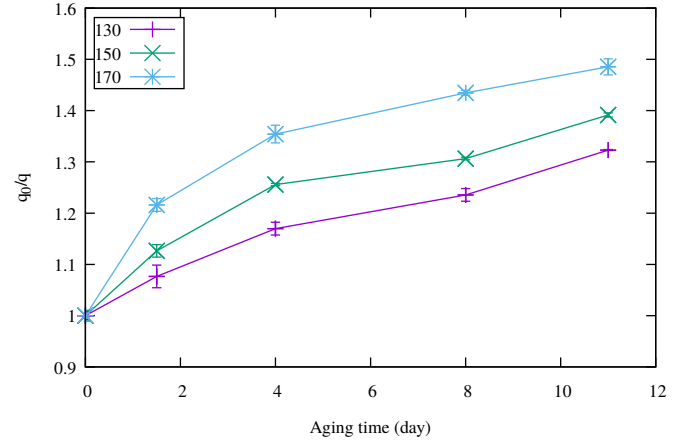


Figure 8: Swelling ratio evolution after aging

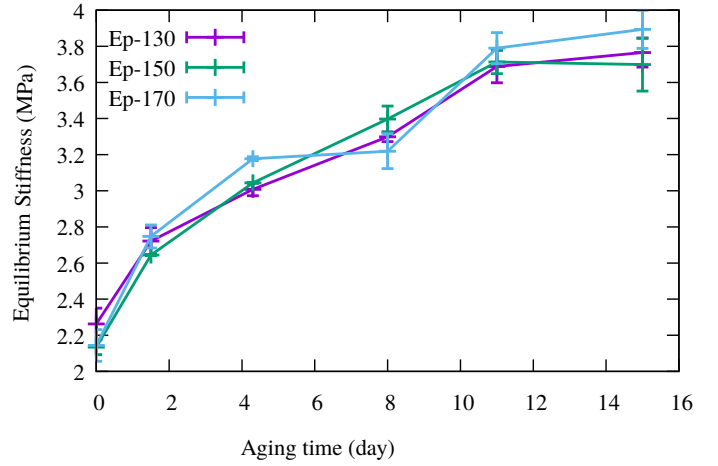


Figure 9: Equilibrium stiffness of aged samples

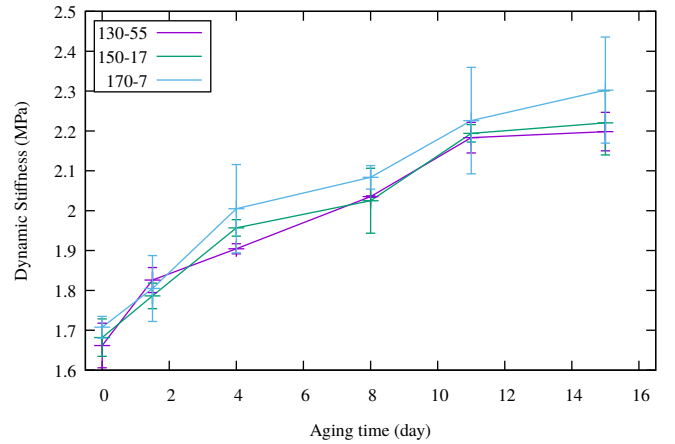


Figure 10: Dynamic stiffness of aged samples (for $f = 10Hz$ at 20% of dynamic amplitude with 30% of static preload)

and the area of stabilized hysteresis curves. In the following, the term dynamic stiffness stands for the median line. Typical results are shown with figures 10 and 11. As for the equilibrium stiffness, the dynamic stiffness increases with aging while the hysteresis area decreases. The dispersion is stronger than for equilibrium results and seems to increase with aging.

Figures 12, 13 and 14 show that the effect of the dynamic amplitude of loading (Payne effect) and the effect of the frequency of loading are not impacted by aging (at least after 15th days of aging): we only see

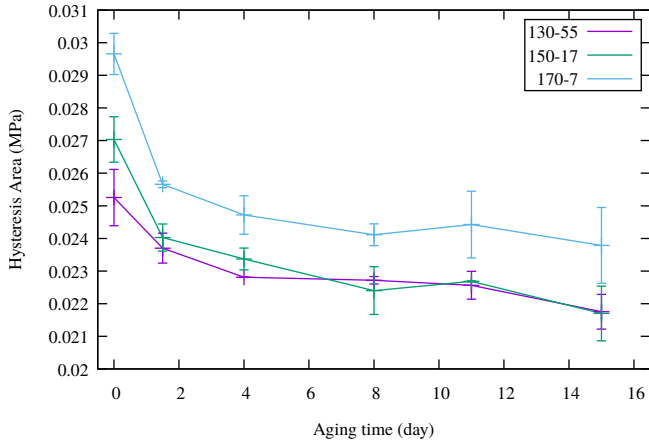


Figure 11: Hysteresis area of aged samples (for $f = 10Hz$ at 20% of dynamic amplitude with 30% of static preload)

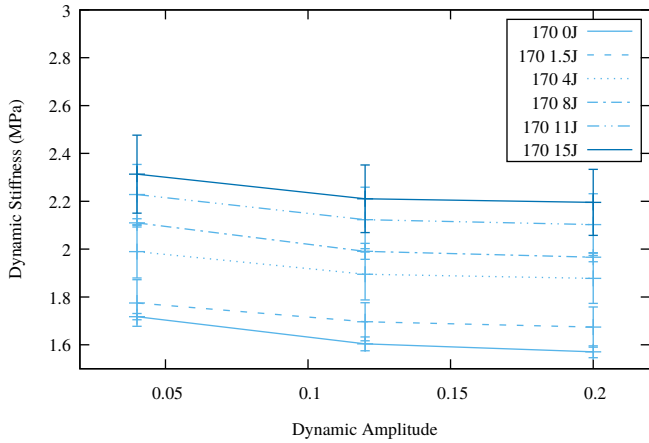


Figure 12: Dynamic stiffness on aged samples upon the amplitude of the dynamic amplitude at 3Hz with 50% of elongation preload

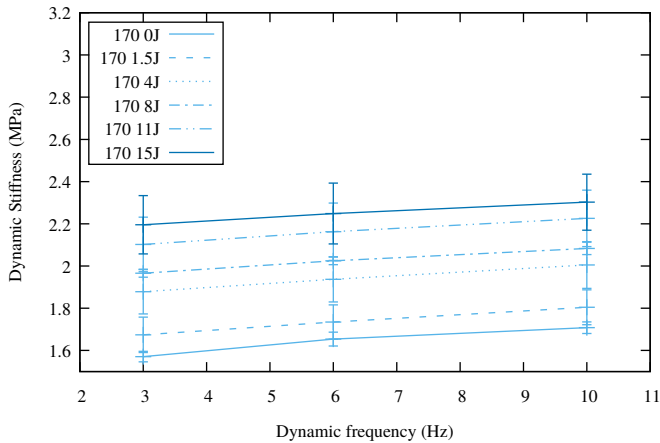


Figure 13: Dynamic stiffness on aged samples upon the amplitude of the dynamic amplitude at 3Hz with 50% of elongation preload

a vertical translation of the curves.

5 DISCUSSION

Based on the previous experimental results we can made the following remarks:

- **Crosslink density and mean crosslink length.** Under non-oxidative conditions, thermal aging leads to an increase of the crosslink density of a sulfur vulcanized filled rubber and this

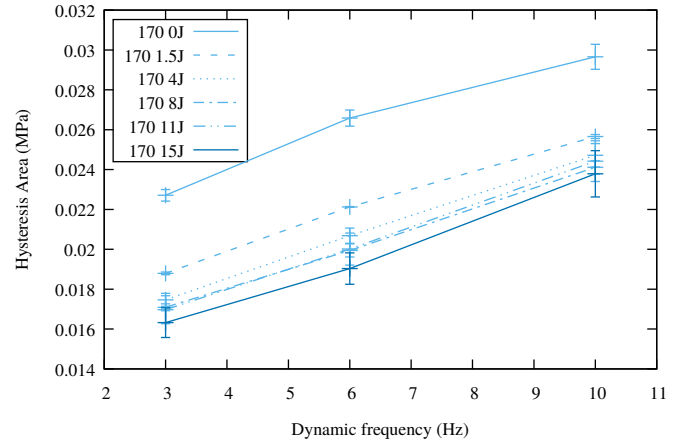


Figure 14: Hysteresis area on aged samples upon the amplitude of the dynamic amplitude at 3Hz with 50% of elongation preload

evolution is related to the initial (and current) mean crosslink length.

- **Fillers/rubber network interactions.** Aging mechanisms seem to not impact in a significant manner the fillers/network interactions (at least at $90^{\circ}C$ for aging). Amplitude and frequency of loading effects are not modified by aging.
- **Rubber network.** The crosslink density may not be the only parameter to take into account in a modeling of non-oxidative aging. In this campaign, we show that the aged mechanical behavior can be slightly different between the three materials even if the results of swelling tests are very close after aging. We guess that the aged rubber network is not exactly the same for the three materials after aging, even if the initial formulation is exactly the same.
- **Dispersion of experimental results.** We saw an increase of the dispersion of experimental results during aging. This effect can have many different origins, this can be due to damage that can occurs during mechanical test. As the limit of chains extensibility is reduced due to aging, damage can occur for smaller load amplitudes. This can also be a consequence of a non homogeneous aging that can have different origins: heterogeneity of temperature in the oven or oxidation (even if we tried to minimize it).

For the modeling part, taking into account of the previous remarks, we will have to introduce at least two supplementary variables that will be related to the mean crosslink length and the crosslink density. We already have introduced a relative crosslink density variable in the unaged behavior (eq. 4). This variable should eventually be complemented with another one.

6 CONCLUSION

We have investigated the consequence of thermal aging for a sulfur vulcanized filled rubber. From the re-

sults of the experimental campaign, we have shown that aging is strongly related to the initial rubber network (crosslink density and mean crosslink length). As already shown by previous authors, the increase of stiffness, the decrease of dissipated energy and the increase of crosslink density are the three main phenomena but the kinetic is dependent on the initial vulcanization system and on the initial crosslink lengths and crosslink densities.

To investigate further aging mechanisms and their kinetic, we need to do other experimental tests with different temperatures of aging. We will also need to study the impact of a permanent mechanical loads during aging, as done by Johlitz, Diercks, & Lion 2014.

From the modeling point of view the challenge is to describe the kinetic with few supplementary variables. We also need to have a good knowledge of the initial network structure and swelling tests may not be sufficient for that.

REFERENCES

- Ben Hassine, M. (2013, October). *Modelling of thermal and mechanical ageings of an external protection of a cold shrinkable junction made of EPDM rubber*. Phd thesis, Ecole nationale supérieure d'arts et métiers - ENSAM.
- Choi, S.-S., J.-C. Kim, & W. C.-S. (2006). Accelerated thermal aging behaviors of epdm and nbr vulcanizates. *Bulletin of the Korean Chemical Society* 27(6), 936 – 938.
- Ciutacu, S., P. Budrugaec, G. Mare, & I. Boconcios (1990). Accelerated thermal ageing of ethylene-propylene rubber in pressurized oxygen. *Polymer Degradation and Stability* 29(3), 321 – 329.
- Delattre, A., S. Lejeunes, F. Lacroix, & S. Méo (2016). On the dynamical behavior of filled rubbers at different temperatures: Experimental characterization and constitutive modeling. *International Journal of Solids and Structures* 90, 178 – 193.
- Flory, P. & J. Rehner (1943). Statistical mechanics of crosslinked polymer networks ii. swelling. *The Journal of Chemical Physics* 11(11), 521–526.
- Gac, P. L., V. L. Saux, M. Paris, & Y. Marco (2012). Ageing mechanism and mechanical degradation behaviour of polychloroprene rubber in a marine environment: Comparison of accelerated ageing and long term exposure. *Polymer Degradation and Stability* 97(3), 288 – 296.
- Johlitz, M., N. Diercks, & A. Lion (2014). Thermo-oxidative ageing of elastomers: A modelling approach based on a finite strain theory. *International Journal of Plasticity* 63, 138 – 151. Deformation Tensors in Material Modeling in Honor of Prof. Otto T. Bruhns.
- Kartout, C. (2016, March). *Thermo-oxidative ageing and fracture behavior of an EPDM*. Phd thesis, Université Pierre et Marie Curie - Paris VI.
- Kraus, G. (1963). Swelling of filler-reinforced vulcanizates. *Journal of Applied Polymer Science* 7, 861–871.
- Kumar, A., S. Commereuc, & V. Verney (2004). Ageing of elastomers: a molecular approach based on rheological characterization. *Polymer Degradation and Stability* 85(2), 751 – 757.
- Rabanizada, N., F. Lupberger, M. Johlitz, & A. Lion (2015). Experimental investigation of the dynamic mechanical behaviour of chemically aged elastomers. *Arch Appl Mech* 85(85), 10111023.
- Shabani, A. (2013, May). *Thermal and radiochemical of neat*

and ATH filled EPDM : establishment of structure/properties relationships. Phd thesis, Ecole nationale supérieure d'arts et métiers - ENSAM.

- Tomer, N., F. Delor-Jestin, R. Singh, & J. Lacoste (2007). Cross-linking assessment after accelerated ageing of ethylene propylene diene monomer rubber. *Polymer Degradation and Stability* 92(3), 457 – 463.